MATERIALS PHYSICS AND MECHANICS RESEARCH ARTICLE

Submitted: February 21, 2026 **Revised: May 12, 2026** **Accepted: May 19, 2026**

Numerical and experimental investigations of the crushing behavior of thin-walled multi-cellular steel cylinders

A.M. Mohebihafshejani, F. Morshedsolouk ✉, A. Moazemi Goudarzi

Babol Noshirvani University of Technology, Babol, Mazandaran, Iran

✉ f.morshed@nit.ac.ir

ABSTRACT

The quasi-static axial crushing behavior of an all-metal corrugated sandwich cylindrical shell is investigated experimentally and numerically. The structure consists of inner and outer thin-walled steel shells connected by a trapezoidal corrugated steel core, fabricated using a low-cost method without adhesives. Quasi-static compression tests were conducted on three ST37 steel specimens and validated using finite element simulations accounting for material plasticity and large deformations. The results show that the corrugated sandwich cylindrical shells deform through stable progressive local buckling. Compared with monolithic cylinders of similar mass, the proposed design exhibits significantly higher energy absorption, reaching up to approximately 1.5 times improvement. Parametric analyses reveal that increasing the number of corrugated units and optimizing the core-to-shell thickness ratio markedly enhance crushing efficiency while reducing peak crushing force. The proposed all-metal corrugated sandwich cylindrical shell provides an efficient, manufacturable solution for lightweight energy-absorbing structures in automotive, marine, and protective engineering applications.

KEYWORDS

metal corrugated sandwich cylindrical shell • thin-walled structures • energy absorption • axial crushing progressive buckling • quasi-static compression

Citation: Mohebihafshejani AM, Morshedsolouk F, Moazemi Goudarzi A. Numerical and experimental investigations of the crushing behavior of thin-walled multi-cellular steel cylinders. *Materials Physics and Mechanics*. 2026;54(4): 134–148.

http://dx.doi.org/10.18149/MPM.5442026_12

Introduction

Crash boxes abilities to improve passengers' safety depends on their capacity to absorb impact energy while maintaining a low impact force. Typical crash boxes are cylindrical or square thin-walled tubes. However, the sandwich cylinders, which have better bending stiffness and buckling strength are studied less than thin-walled tubes, and there is a gap in understanding the axial crushing behavior of steel thin-walled sandwich panes.

Alexander [1] pioneered the field of quasi static crushing of cylinders by introducing a mathematical model to calculate the average crushing force of pipes exhibiting progressive buckling mode in axially symmetric deformation. Since then, researchers have focused on the energy-absorption capabilities of thin-walled cylinders by decreasing peak crushing force (PCF) and increasing energy absorption capability (EA). For example, Rahi [2] used numerical analysis and laboratory tests and demonstrated that, despite the lower absorbed energy, circular coaxial double-walled tubes, compared to square tubes, exhibit a higher specific absorbed energy (SAE). Completing their finding, Alavi Nia and Hamedani [3] conducted a numerical simulation of various aluminum tubes, including

© A.M. Mohebihafshejani, F. Morshedsolouk, A. Moazemi Goudarzi, 2026.
Publisher: Peter the Great St. Petersburg Polytechnic University
This is an open access article under the CC BY-NC 4.0 license (https://creativecommons.org/li-censes/by-nc/4.0/)

cylindrical, hexagonal, pyramidal, conical, and rectangular shapes, and concluded that cylindrical tubes exhibited the highest energy absorption capacity. In contrast, Marzbanrad et al. [4] suggested that pipes with an oval cross-section possess a greater energy absorption capacity compared to square or circular tubes. In a separate study, Zhang et al. [5] numerically investigated the compression behavior of two types of pyramidal square tubes and found that they exhibited improved energy absorption capacities ranging from 15 to 33 % and 54 to 93 % compared to standard square tubes. Finally, Hosseinpour et al. [6] studied the behavior of cylinders with auxetic pattern cut and stated that the porosity and auxetic pattern are the most prominent parameters in the crashworthiness of these structures. Sandwich cylinders have a greater overall bending stiffness, which effectively prevents the global buckling mode. Moreover, the core and its interaction with the shells of the faceplate enhance the energy absorption capacity of the sandwich structures (Lu et al. [7]). As a result, sandwich structures have gained attention as energy-absorbing structures in many recent studies. For instance, Su et al. [8] investigated the crushing behavior of foam-filled corrugated sandwich cylindrical shells under axial compression using theoretical and numerical methods and reported a maximum specific energy absorption of 60 kJ/kg with a coupling strengthening effect of up to 40 %. Agarwal and Sobelt [9] conducted an optimization study on stiffened and unstiffened composite sandwich cylindrical shells and discovered that sandwich shells featuring graphite/epoxy surfaces and aluminum honeycomb cores offer a higher weight efficiency across various external loads. Hutchinson and He [10] investigated the buckling optimization of cylindrical sandwich shells filled with metal foam and found that cylindrical sandwich shells offer a similar weight advantage to stringer-reinforced shells. In another study, Yang et al. [11] investigated the free vibration and axial compression of all-metal cylindrical and truncated conical sandwich shells with corrugated cores numerically and experimentally. Their findings demonstrated that the load-carrying capacity (i.e., maximum crushing force) of a conical or cylindrical sandwich shell can be significantly enhanced through optimization when the first natural frequency must be within a specific range. More recently, Yang et al. [12] suggested that by prefabricating circumferential band defects in corrugated sandwich cylindrical shells, it is possible to decrease the PCF, while the energy absorption capacity will not change.

The energy absorption of the multicell and foam-filled cylinders was also investigated. For example, Alavinia and Parsapour [13] examined the energy absorption capacity of multicellular structures with regular polygonal sections. They demonstrated that multicellular structures are an effective method for improving and strengthening mechanical properties. Specifically, multicellular sections absorb more energy than simple sections, and hexagonal and octagonal sections absorb more energy per unit mass. Similarly, Yan et al. [14] investigated the energy absorption characteristics of flax fiber composite tubes filled with polyurethane foam when subjected to quasi-static axial compressive load. Likewise, Tang et al. [15] conducted numerical studies on circular multi-cell tubes and demonstrated that circular multi-cell tubes possess greater energy absorption capacity than square cross-section tubes. Additionally, the energy absorption of 3D-printed polymer and fiber-reinforced cellular structures has been extensively explored through analytical, numerical, and experimental methods, including scutoid cellular geometries [16], kite-shaped [17], sinusoidal [18], double octagonal bipyramid [19], bone-

inspired [20], auxetic honeycomb [21], hybrid surface-strut [22], lozenge grid [23], bi-material quadrilateral bipyramid [19], and hybrid cellular [24] configurations.

The studies on sandwich structures of metal cylinders are limited. For example, Zhang et al. [25] developed an analytical model to predict the failure mode of the all-metallic sandwich cylinders with square honeycomb cores under axial compression. Some researchers suggested that foam or honeycomb-filled sandwich cylindrical shells have better axial compressive performance [26–31]. These studies have demonstrated that sandwich panels utilizing 3D truss or 2D prismatic cores exhibit comparable or greater weight reduction and design advantages than foam/honeycomb sandwich panels [32–34]. Corrugated sandwich structures with open-core topologies have the potential to serve as thermal protection systems for manned spacecraft, offering thermal protection and load-bearing capabilities for the outer covering [35].

The side shells and corrugated core of the sandwich cylinders absorb energy through progressive local buckling. Because the corrugated core controls the deformation of the inner and outer shell cylinders, the folds created in the body of this structure are smaller than those created in thin-walled cylinders and require more energy to form. Therefore, researchers have focused on these structures. Fan et al. [35] and Chen et al. [24] constructed CFRC GSCs with Kagome lattice cores. They found that fluted-core composite structures may be advantageous for specific launch vehicle structures. The stiffness, strength, and modal response of composite sandwich cylinders have been widely studied [36–41]. Zhang et al. [42,43], Liu et al. [44], and Peng-Bo et al. [45] studied the buckling and collapse behaviors of all-metal sandwich cylindrical shells. Zhang et al. [42,43] conducted numerical investigations to analyze the energy absorption capacity of Kagome aluminum honeycomb sandwich cylindrical columns and compare them to cylindrical columns filled with aluminum foam under axial crushing loads. Nevertheless, their research solely utilized the finite element method and did not involve the construction and testing of sandwich structures. Li et al. [44] designed and manufactured a large-scale sandwich cylinder with a corrugated core using carbon fiber-reinforced composites and examined its resistance and failure modes. Wang at al. [46] reviewed the application and mechanical applications of multicellular cylinders, and highlighted their energy absorption capabilities.

In this paper, a cylindrical sandwich shell with a corrugated metal core was developed and its axial crushing behavior was investigated. Despite extensive research on thin-walled and sandwich cylinders, no experimental study has investigated the influence of corrugation angle on the axial crushing behavior of friction-fit (adhesive-free) corrugated sandwich cylinders. The proposed manufacturing method reduces production costs by eliminating the adhesive bond between the shell and core plates and relying on frictional forces. Three test specimens with different core angles were fabricated and tested. Their crushing loads and failure modes were then examined. The aim of this study is to evaluate the influence of the core-to-plate thickness ratio ($\frac{t_c}{t_f}$), corrugation angle (α), and the number of corrugated units (n) on the crushing behavior of the sandwich cylinders.

Materials and Methods

The crushing behavior of the steel corrugated sandwich cylindrical shells is studied experimentally and numerically. Three steel corrugated sandwich cylindrical shells were fabricated using a straightforward and cost-effective method that eliminates the need for adhesives. The specimens were subjected to a quasi-static compression test until the densification stage. These corrugated sandwich cylindrical shells consist of a thin-walled outer shell, a thin-walled inner shell, and a thin-walled corrugated core, as shown in Fig. 1.

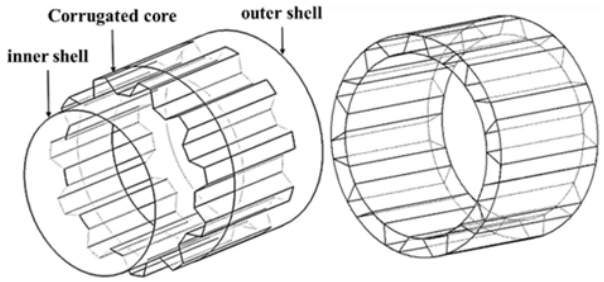


Fig. 1. Schematic representation of the corrugated sandwich cylindrical shell geometry

Specimens' fabrication and experimental setup

To fabricate the test specimens a trapezoidal corrugated core was formed using a bending machine to create the desired profile. The trapezoidal core was rolled into a cylindrical shape using a custom cylindrical mould. The edges were welded to ensure structural continuity and stability. Inner and outer cylindrical shells were fabricated by cutting steel sheets into rectangles using a guillotine machine, with dimensions based on the targeted radius. The sheets were rolled into cylindrical shapes and spot-welded at eight uniformly distributed points along the edges. The corrugated core was integrated between the inner and outer shells, completing the assembly. ST37 (ASTM A 283 M-98) construction steel was selected for all the components due to its ease of machining, good formability, high yield stress, and high tensile strength. The mechanical properties of ST37 steel were determined through tensile testing, in accordance with ASTM E8/E8M-13a. Test samples were laser-cut to specified dimensions, with gauge lengths measured using a calliper before testing. Each sample underwent tensile loading until failure, and the resulting stress-strain curve is shown in Fig. 2.

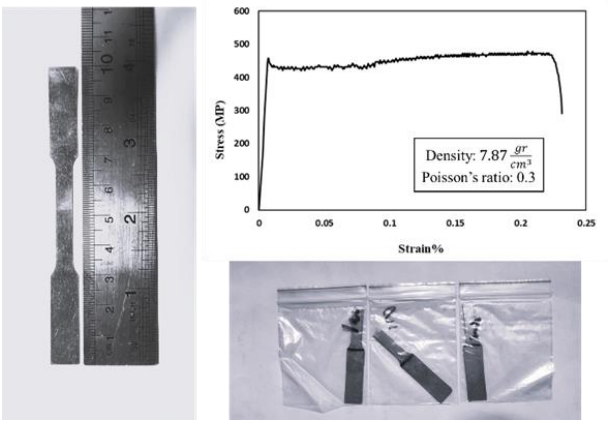


Fig. 2. Tensile stress–strain curve of ST37 steel, along with specimens before and after tensile testing

The corrugated cores had a trapezoidal profile, and the geometric parameters of the corrugated sandwich cylindrical shells are illustrated in Fig. 3. All specimens shared consistent dimensions, of height (h = 120 mm), outer shell radius (R_O=180 mm), and inner shell radius (R_i = 150 mm). The number of corrugated units in the core varied among specimens, as listed in Table 1. The final fabricated models are shown in Fig. 4.

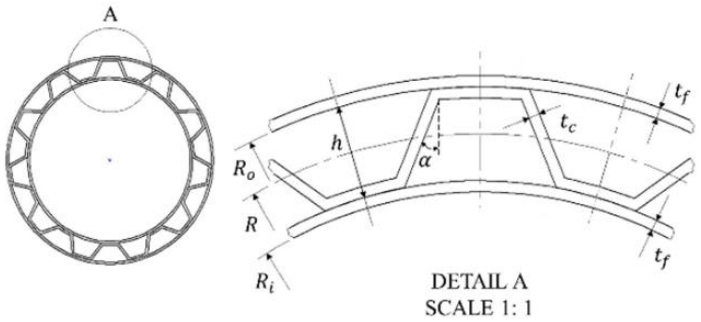


Fig. 3. Geometrical parameters defining the corrugated sandwich cylinders

Table 1. Geometric parameters for the experimental and FEM specimens

Geometric parameters	***n***	***h*, mm**	***R_i*, mm**	***R_0*, mm**	**t_c, mm**	**t_f, mm**	**α, °**	**Type**
TMCS10	13	120	150	180	0.2	0.2	10	Exp + Num
TMCS25	11	120	150	180	0.2	0.2	25	Exp + Num
TMCS40	8	120	150	180	0.2	0.2	40	Exp + Num
CSCS0	11	120	150	180	0.2	0.2	0	Num
CSCS25* (TMCS25)	11	120	150	180	0.2	0.2	25	Exp + Num
CSCS55	11	120	150	180	0.2	0.2	55	Num
TMCS25_1	11	120	150	180	0.2	0.1	25	Num
TMCS25_2* (TMCS25)	11	120	150	180	0.2	0.2	25	Exp + Num
TMCS25_3	11	120	150	180	0.1	0.2	25	Num
TMCS25_4	11	120	150	180	0.06	0.2	25	Num

* these specimens are the same as TMCS25

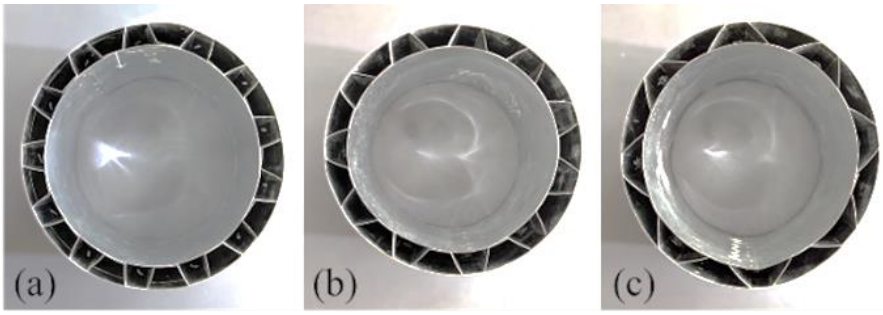


Fig. 4. Manufactured corrugated sandwich cylindrical specimens: (a) TMCS10, (b) TMCS25, and (c) TMCS40

The fabricated steel corrugated sandwich cylindrical shells are subjected to quasi-static compressive load using the STD600 hydraulic testing machine. First, the specimen was placed between two platens of the machine with a constant rate of 1 mm/min. The force-displacement curves and deformation modes are extracted for each specimen.

Finite element modeling

Finite element (FE) analysis was employed to simulate the crushing behavior of the corrugated sandwich cylindrical shells. The explicit solution method was used to address the highly nonlinear nature of the problem, which involves large deformations, buckling, and material nonlinearity. The FE model included the inner and outer shells, corrugated core, and the platens of the test machine (Fig. 5). The shells and core were modelled using four-node shell elements (S4R) with five integration points through the thickness. The rigid platens were represented using four-node rigid elements (R3D4) with dimensions of 2×2 mm^2 [45]. General contact is implemented in all models, with a constant Coulomb friction coefficient of 0.2. Axial loading is applied by gradually moving the upper rigid plate to simulate quasi-static loading, while the lower rigid plate is fixed. Axial loading is applied by gradually moving the upper rigid plate to simulate quasi-static loading, while the lower rigid plate is fixed. To validate the quasi-static loading condition the criterion presented by Santosa et al. [47] is checked; during the during simulated crushing, the ratio of the total kinetic energy to total internal energy remains smaller than 2 %, and the force response and displacement remain unaffected by the applied speed. The ST37 steel plates were modeled as an isotropic elastic-plastic solid under von Mises J2 flow theory and the material data is from the engineering stress-strain curves in Fig. 2. For mesh convergence, the TMCS25 specimen was simulated using various mesh sizes. According to the graph presented in Fig. 6, the mesh size of 1 mm is chosen for the simulations.

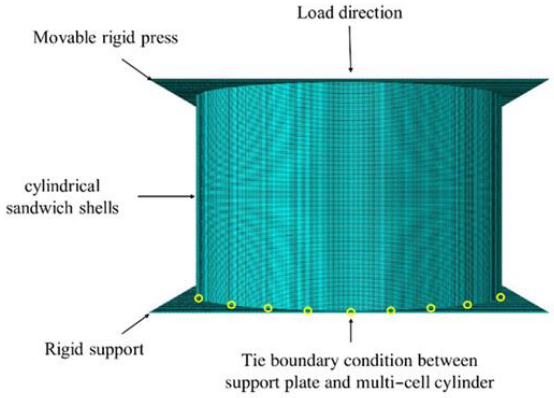


Fig. 5. Meshed model of the corrugated sandwich cylindrical shell showing the applied boundary and loading conditions

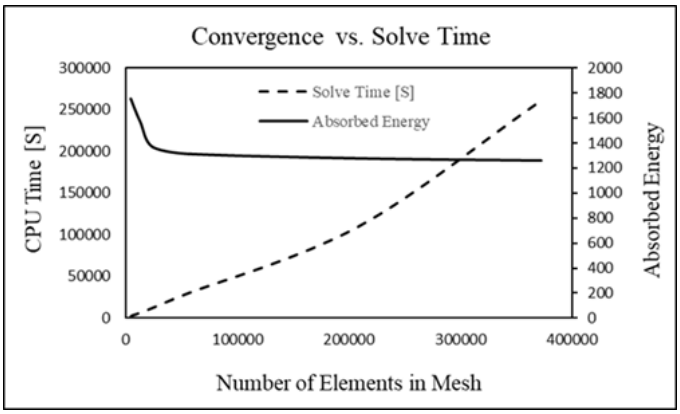


Fig. 6. Convergence and mesh dependency chart with solution time for the TMCS25 model

Results and Discussion

In this study, first three quasi-static compression tests were conducted, and results were used to validate the finite element model. Then, a parametric study was conducted using the FE model to investigate the effect of the core-to-plate thickness ratio on the initial compressive failure load.

Validation

To validate the finite element model, the results of the test specimens crushing are modeled in ABAQUS/EXPLICIT and the results are compared to the test results. The force–displacement responses of TMCS10, TMCS25, and TMCS40 from experiments and numerical analysis are presented in Fig. 7. Overall, a satisfactory agreement between simulations and experiments is observed, confirming the validity of the finite element model. For all specimens the errors for the PCF and MCF are below 15 %, although for the TMCS10 specimens the local error in the plateau region is higher. Minor discrepancies are mainly attributed to manufacturing imperfections, including spring-back effects

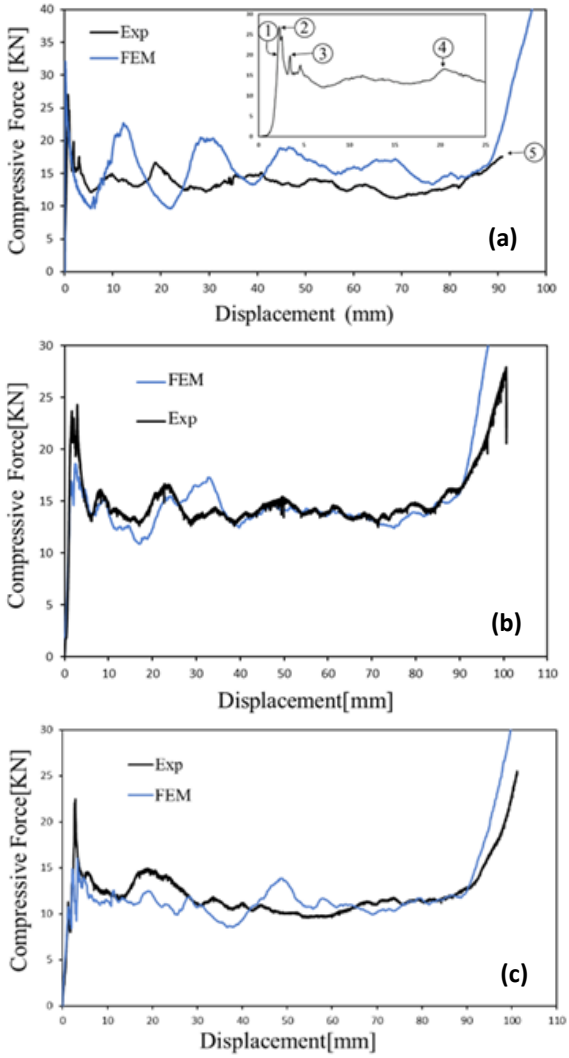


Fig. 7. Force-displacement curves for corrugated cylindrical sandwich specimens: (a) TMCS10, (b) TMCS25, (c) TMCS40

during forming, local bending of intermediate meshes, non-uniform weld dimensions, and possible local separation between the shell and the core during deformation.

The TMCS10 model has more corrugated units in the core, the local folds in the faceplates are smaller and the error may be attributed to the sensitivity of the model to these small variations. On the other hand, increasing the number of corrugated units in the core improves the load-bearing capacity and energy absorption of the specimens, in experiment results. Compared to a similar specimen with fewer corrugated units in core, the absorbed energy increased by up to 1.51 times for TMCS10, while the overall weight remained nearly unchanged. In both experiments and the numerical analysis, the dominant failure mode was asymmetric progressive folding, known as diamond progressive folding.

For the TMCS10 model, the response is initially linear elastic until the peak crushing force (PCF = 26.9 kN) is reached. Beyond this point, progressive buckling occurs, leading to repeated load fluctuations associated with fold formation. During testing, the TMCS10 specimen experienced four main buckling events. A similar initial elastic behavior is observed for the TMCS25 model, with a lower peak crushing force of PCF = 17.1 kN.

The initiation and evolution of buckling in the TMCS10 specimen are marked by points 1 to 5 in Fig. 7(a), with the corresponding deformation states illustrated in Fig. 8. The first half-wave forms slightly before the initial peak load and subsequently propagates around the cylinder circumference. Each newly formed half-wave corresponds to a local peak in the force–displacement curve, while the final stage represents complete compression of the structure.

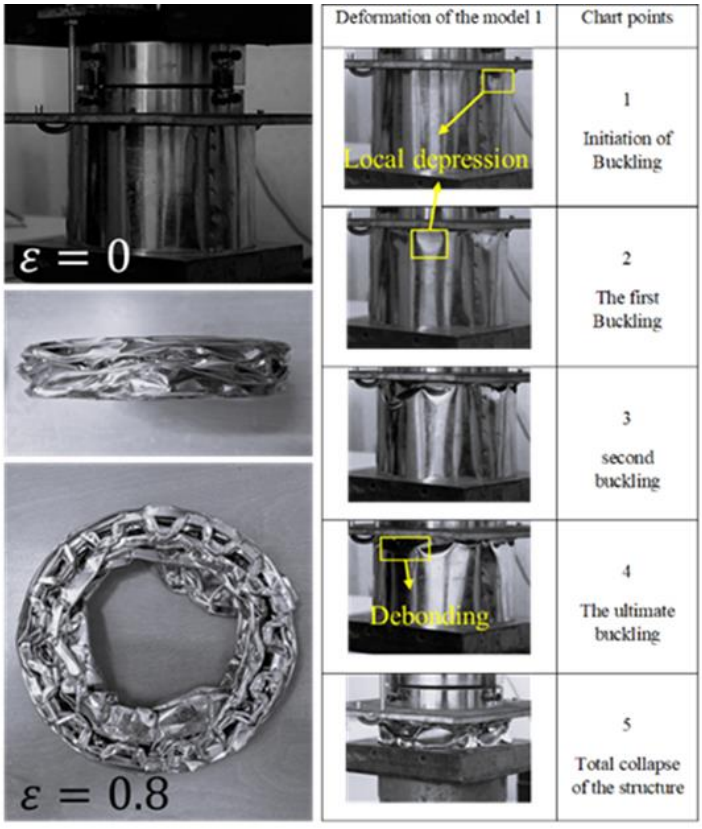


Fig. 8. Key buckling modes of the TMCS10 corrugated sandwich cylindrical shell, highlighting the critical deformation patterns under axial compression

The absorbed energy during crushing was determined from the area under the force–displacement curves. The ultimate strength and absorbed energy values for all specimens are summarized in Table 2. The TMCS10 model exhibits the highest peak crushing force and energy absorption due to the larger number of corrugated units in core, despite having approximately the same weight as the other specimens.

Table 2. Ultimate strength and energy absorption of the corrugated sandwich cylindrical shell for the experimental models TMCS10, TMCS25, and TMCS40

	TMCS10	**TMCS25**	**TMCS25**
PCF, kN	28.84	24.32	22.48
EA, J	1567	1280	1040

Initial collapse and crushing response

This section presents an analysis of the initial collapse and crushing response of corrugated sandwich cylindrical shells based on numerical simulations, with the TMCS25 model discussed for conciseness. Figure 9 shows the force–displacement response of

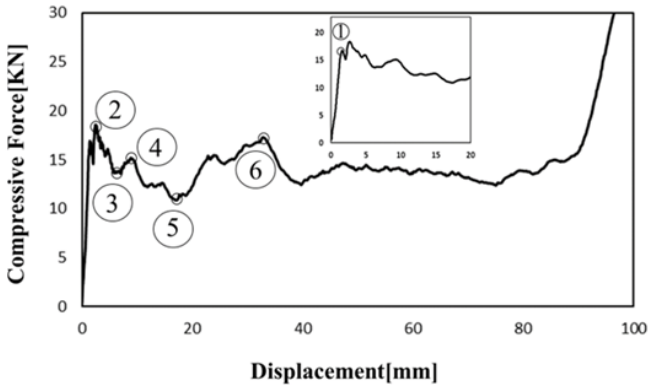


Fig. 9. Force–displacement curve of TMCS25 from FEM model

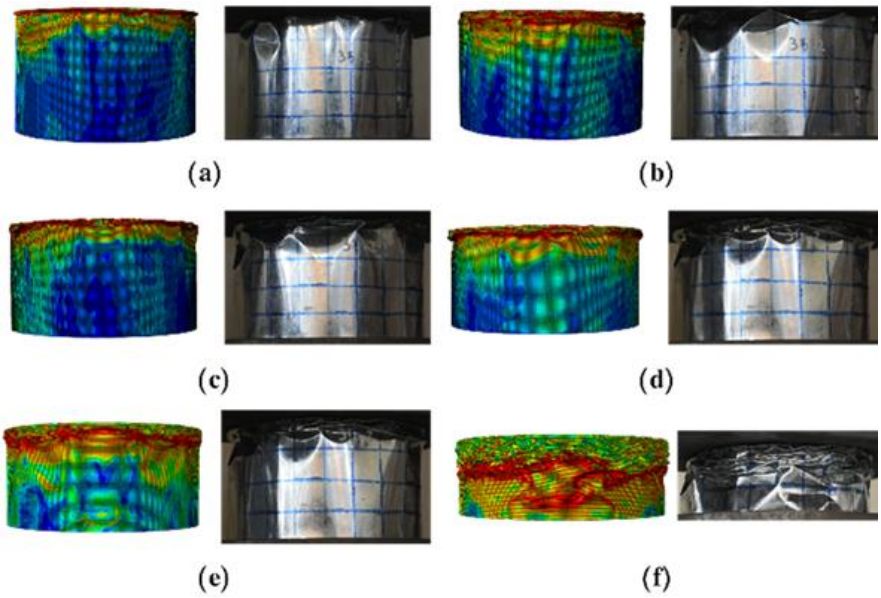


Fig. 10. Comparison of experimental and finite element failure modes of the TMCS25 corrugated sandwich cylindrical shell at different stages of axial crushing: (a) initial collapse; (b) first fold in the outer shell; (c)completion of first fold; (d) completion of first fold; (e) second fold; (f) last fold

the corrugated sandwich cylindrical shell. The initial collapse stage includes the elastic response and the onset of failure, followed by a crushing stage characterized by complex plastic deformation and progressive fold formation. A comparison between experimental and numerical failure modes for TMCS25 is provided later in Fig. 10.

The initial collapse response extends from the origin to point 2 in Fig. 9. The force–displacement curve remains nearly linear up to point 1. As this point is approached, lateral deflection of the corrugated core increases, resulting in localized buckling. This deformation mode, referred to as localized buckling in this study, causes the corrugated core to bend inward toward the inner shell along a circumferential line and detach locally from the inner shell, as shown in Fig. 11.

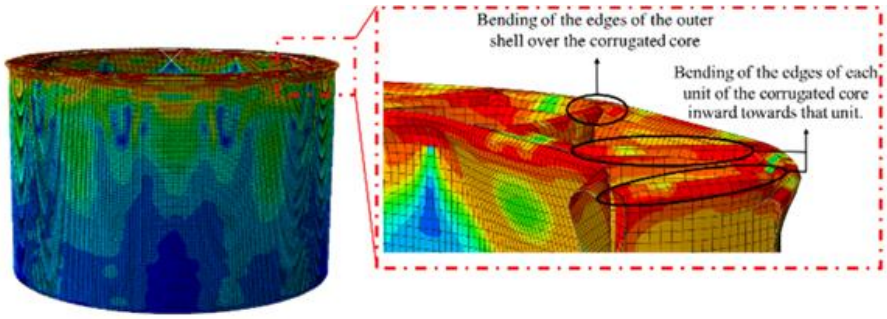


Fig. 11. Response of the delamination of the TMCS25 sandwich shell at point 2

After point 1, the crushing force dropped as plastic deformation spreads in the core and yielding initiates in the sheets. With further downward movement of the pressing platen, the outer shell bends inward toward the core, as illustrated in Fig. 11, the core and the inner shell separated locally at the top. The edge of the inner shell bends outward, leading to the formation of the first fold and causing the crushing force to increase and reaching to point 2 in Fig. 9.

After fold formed, there is a sudden load drop. During this stage, yielding of the plates and post-buckling of the core occur simultaneously. At point 3, the next row of folds starts to take place, and at point 4 these folds are completed. At point 5 the third row of folds start. As the response approaches point 6 in Fig. 9, buckling of sandwich cylinder is completed. The buckling deformation in the corrugated core penetrates into the plate buckling region, indicating strong interaction between the core and shell components.

Effect of geometric parameters

The effects of the core-to-plate thickness ratio (t_c/t_f) and corrugation angle (α) on the crushing behavior of the sandwich panels are studied using the finite element method. Figure 12 presents the force–displacement curves of specimens with different core-to-plate thickness ratios $\left(t_c/t_f = 2,\ 1,\ 0.5,\ 0.3\right)$. In this analysis corrugation angle for all specimens is of 25°. The material of all components was mild steel, and the geometric details are summarized in Table 1. The overall trends of the curves are similar, but for lower thickness ratio, the peak crushing force (PCF) is smaller. For instance, the initial model TMCS25_2 exhibits a peak force of 24.32 kN, whereas this value decreases to 12.84 kN for the TMCS25_3 model.

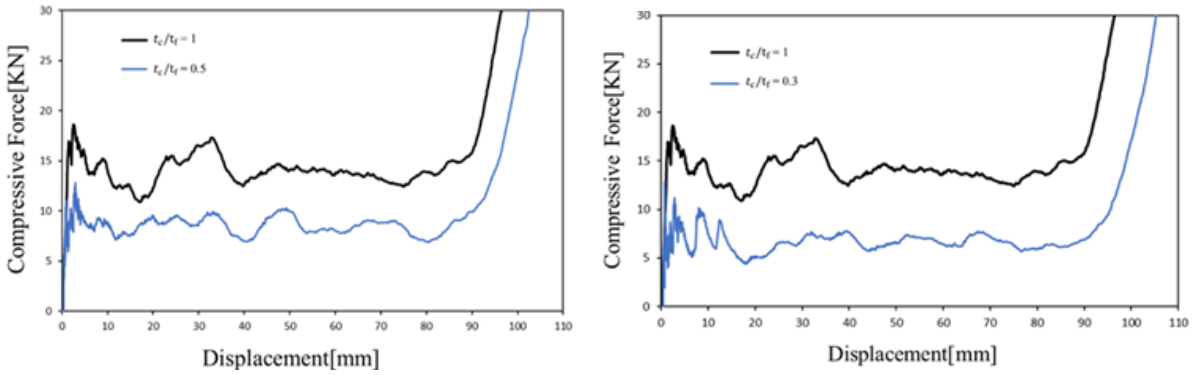


Fig. 12. Force-displacement curves of thin-walled multi-cellular steel cylinders with varying core-to-shell thickness ratios: (a) $^{t_c}/_{t_f} = 0.5$ and $^{t_c}/_{t_f} = 1$; (b) $^{t_c}/_{t_f} = 0.3$ and $^{t_c}/_{t_f} = 1$

This reduction in PCF is attributed to the triggering of buckling, which lowers the structural stiffness and facilitates crushing. In contrast, a marked increase in PCF is observed when both the core and shell thicknesses are 2 mm $\left(t_c/t_f = 1\right)$, owing to the increased stiffness associated with thicker walls. A similar trend is observed for the mean crushing force (MCF), which increases with thickness. Moreover, the energy absorption (EA) and specific energy absorption (SEA) reach their maximum values at $t_c/t_f = 1$. Although thicker walls increase the mass of the structure, the corresponding increase in absorbed energy dominates, resulting in higher SEA.

To evaluate the effect of the corrugated core angle on the crushing response, it is important to note that changing the angle alters the number of corrugated units in both experimental and numerical models. Therefore, in this section, the number of corrugated units was kept constant at $N = 11$, and two angles, 0° and 55°, were considered. The model dimensions were fixed at a height of 120 mm, inner and outer radii of 75 mm and 90 mm, respectively, with a uniform three-layer thickness of 2 mm. The CSCS25 model (25°) was selected as the reference case and was also tested experimentally, whereas CSCS0 and CSCS55 were analyzed numerically only. Figure 13 shows the crushing force–displacement curves obtained from finite element simulations for the different core angles.

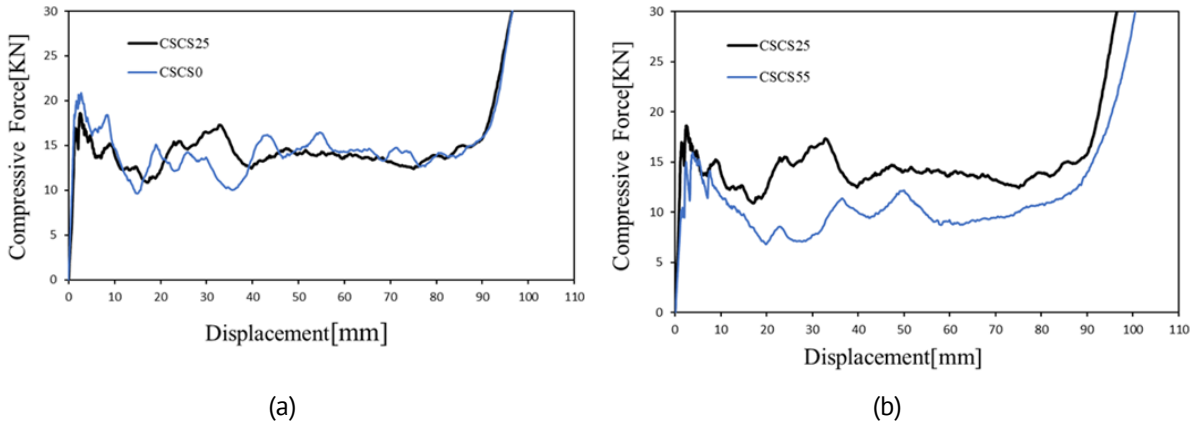


Fig. 13. Crushing force-displacement curves of thin-walled multi-cellular steel cylinders with varying core angles: (a) CSCS25 and CSCS0; (b) CSCS25 and CSCS55

Figure 14 provides a comparative overview of the effects of core angle and thickness ratio on the main crushing indices. Each bar chart represents one energy absorption index, with the left side corresponding to variations in the core angle α (see Fig. 3) and the right-side representing changes in the thickness ratio. All results are reported for $N = 11$. When the angle varies, the thickness ratio is fixed at 1, and when the thickness ratio varies, the angle is maintained at 25°. The model with $t_c/t_f = 0.3$ exhibits the lowest PCF. However, the model with $t_c/t_f = 1$ achieves the highest energy absorption, specific energy absorption, and crushing force efficiency.

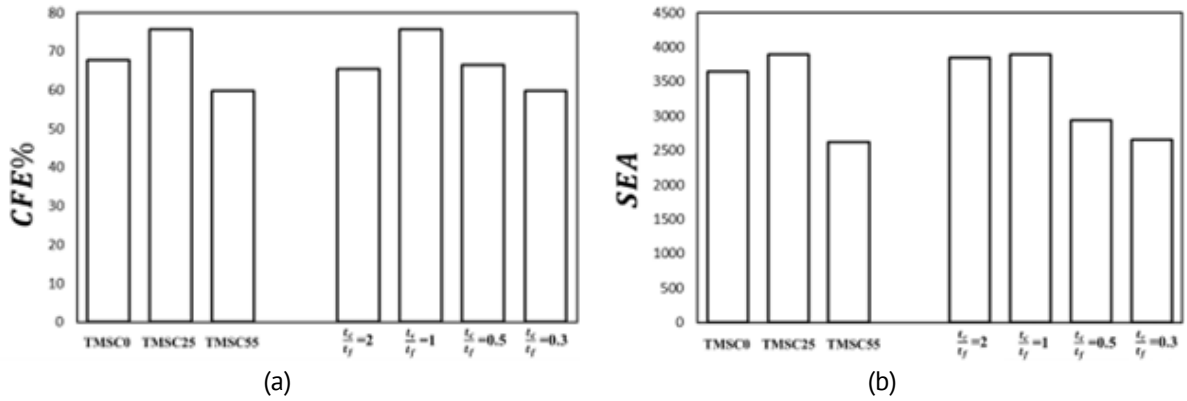


Fig. 14. Variation of specific energy absorption (SEA) and crushing force efficiency (CFE) with core angle and core-to-plate thickness ratio: (a) CFE; (b) SEA

Conclusion

This study investigated the axial crushing behavior and energy absorption performance of corrugated sandwich cylindrical shells using experimental tests and finite element simulations. Three specimens were tested to identify the dominant deformation mechanisms and to validate the numerical model, which showed good agreement with experimental force–displacement responses and failure modes.

The results indicate that the structures predominantly collapse through asymmetric progressive axial folding initiated by local wall buckling, while Euler and axisymmetric buckling were not observed. The interaction between the corrugated core and the cylindrical shells significantly enhances crushing stability and energy absorption. Increasing the number of corrugated units in core improves the load-bearing capacity and absorbed energy, achieving up to a 1.51-fold increase without a noticeable change in weight.

Parametric analyses demonstrated that geometric parameters strongly influence the crushing response. The core-to-plate thickness ratio governs the peak crushing force and energy absorption indices, with the highest energy absorption and specific energy absorption occurring at $t_c/t_f = 1$. Although larger corrugation angles reduce the initial buckling force, they also decrease crushing efficiency and specific energy absorption. Among the investigated configurations, the TMCS25 model provides a balanced combination of triggering load and energy absorption performance.

Overall, the results confirm the effectiveness of corrugated sandwich cylindrical shells as energy-absorbing structures and provide useful design guidance for optimizing their geometric parameters in crashworthiness applications.

CRediT authorship contribution statement

Mohebihafshejani Ashkan: investigation, software, formal analysis, validation, writing – original draft; **Morshedsolouk Fattaneh**: conceptualization, methodology, data curation, supervision, writing – review & editing; **Moazemi Goudarzi Ali**: conceptualization, methodology, data curation, supervision.

Conflict of interest

The authors declare that they have no conflict of interest.

This manuscript was edited for language and clarity with the assistance of AI-based tools. The authors have carefully reviewed all content and confirm that all data, analyses, interpretations, and conclusions are original and entirely the work of the authors. No scientific results were generated or fabricated by AI.

References

1. Alexander JM. An approximate analysis of the collapse of thin cylindrical shells under axial loading. *The Quarterly Journal of Mechanics and Applied Mathematics.* 1960;13(1): 10–15.
2. Rahi A. Controlling energy absorption capacity of combined bitubular tubes under axial loading. *Thin-Walled Structures.* 2018;123: 222–231.
3. Nia A, Hamedani J. Comparative analysis of energy absorption and deformations of thin-walled tubes with various section geometries. *Thin-Walled Structures.* 2010;48(12): 946–954.
4. Marzbanaad J, Mehdikhanlo M, Pour AS. An energy absorption comparison of square, circular, and elliptic steel and aluminum tubes under impact loading. *Turkish Journal of Engineering and Environmental Sciences.* 2009;33(3): 159–166.
5. Zhang X, Cheng G, You Z, Zhang H. Energy absorption of axially compressed thin-walled square tubes with patterns. *Thin-Walled Structures.* 2007;45(9): 737–746.
6. Hosseinpour E, Goudarzi AM, Morshedsolouk F, Gharehbaghi H. Numerical and experimental study on the energy absorption characteristics of thin-walled auxetic cylindrical tubes with varying porosity. *Journal of Materials Research and Technology.* 2025;39: 400–417.
7. Taghipoor H, Damghani Nouri M. Axial crushing and transverse bending responses of sandwich structures with lattice core. *Journal of Sandwich Structures & Materials.* 2020;22(3): 572–598.
8. Su P, Han B, Wang Y, Wang H, Gao B, Lu TJ. Crashworthiness of Foam-Filled Cylindrical Sandwich Shells with Corrugated Cores. *Materials.* 2023;16(19): 6605.
9. Agarwal SS, Kansal ML. Weight Comparisons of Optimized Stiffened, Unstiffened, and Sandwich Cylindrical Shells. *Journal of Aircraft.* 1977;14(10): 1000–1008.
10. Hutchinson JW, He MY. Buckling of cylindrical sandwich shells with metal foam cores. *International Journal of Solids and Structures.* 2000;37(46-47): 6777–6794.
11. Mao Y, Han B, Su PB, Wei ZH, Zhang Q, Zhang QC, Lu TJ. Free vibration and axial compression of all-metallic cylindrical and truncated conical sandwich shells with corrugated cores. *Journal of Sandwich Structures & Materials.* 2021;23(6): 2274–2295.
12. Yang M, Mao Y, Zhang J, Han B. Enhancement of artificial defects on the crashworthiness of corrugated sandwich cylindrical shells. *Engineering Structures.* 2025;339: 120658.
13. Nia AA, Parsapour M. Comparative analysis of energy absorption capacity of simple and multi-cell thin-walled tubes with triangular, square, hexagonal and octagonal sections. *Thin-Walled Structures.* 2014;74: 155–165.
14. Yan L, Chouw N, Jayaraman K. Effect of triggering and polyurethane foam-filler on axial crushing of natural flax/epoxy composite tubes. *Materials & Design (1980-2015).* 2014;56: 528–541.
15. Tang Z, Liu S, Zhang Z. Analysis of energy absorption characteristics of cylindrical multi-cell columns. *Thin-Walled Structures.* 2013;62: 75–84.

16. Sepahvand Y, Farrokhabadi M, Moazemi Goudarzi A. Experimental and numerical study of energy absorption in bio-inspired scutoid cellular structures. *Materials Physics and Mechanics.* 2025;53(6): 63–81.
17. Musavi A, Gharehbaghi H, Farrokhabadi A, Sadeghzade M, Hedayati SK, Behravesh AH. Investigation of the equivalent mechanical and thermal properties of the kite-shaped fiber-reinforced cellular structure: Analytical, numerical and experimental approaches. *Engineering Structures.* 2025;337: 120517.
18. Avarzamani M, Gharehbaghi H, Bahrami M, Farrokhabadi A, Behravesh AH, Hedayati SK. Energy absorption response of functionally graded 3D printed continuous fiber reinforced composite cellular structures: Experimental and numerical approaches. *Mechanics of Advanced Materials and Structures.* 2025;32(4): 538–554.
19. Gharehbaghi H, Farrokhabadi A. Experimental, analytical, and numerical studies of the energy absorption capacity of bi-material lattice structures based on quadrilateral bipyramid unit cell. *Composite Structures.* 2024;337: 118042.
20. Ghorbani F, Gharehbaghi H, Farrokhabadi A, Bolouri A, Behravesh AH, Hedayati SK. Investigation of energy absorption performances of a 3D printed fiber-reinforced bio-inspired cellular structure under in-plane compression loading. *Mechanics of Advanced Materials and Structures.* 2024;31(21): 5234–5252.
21. Farrokhabadi A, Veisi H, Gharehbaghi H, Montesano J, Behravesh AH, Hedayati SK. Investigation of the energy absorption capacity of foam-filled 3D-printed glass fiber reinforced thermoplastic auxetic honeycomb structures. *Mechanics of Advanced Materials and Structures.* 2023;30(4): 758–769.
22. Gharehbaghi H, Farrokhabadi A, Noroozi Z. Introducing a new hybrid surface strut-based lattice structure with enhanced energy absorption capacity. *Mechanics of Advanced Materials and Structures.* 2024;31(14): 2955–2964.
23. Gharehbaghi H, Jamshidi M, Almomani A. Experimental and numerical investigation of energy absorption in honeycomb structures based on lozenge grid unit cells under various loading angles. *Composites Part C: Open Access.* 2024;15: 100546.
24. Ghorbani F, Gharehbaghi H, Farrokhabadi A, Bolouri A.Evaluation of the mechanical properties and energy absorption in a novel hybrid cellular structure. *Aerospace Science and Technology.* 2024;148: 109105.
25. Zhang Z, Wang Y, Huang L, Fu Y, Zhang Z, Wei X, Sui Y, Zhang Q, Jin F. Mechanical behaviors and failure modes of sandwich cylinders with square honeycomb cores under axial compression. *Thin-Walled Structures.* 2022;172: 108868.
26. Budiansky B. On the minimum weights of compression structures. *International Journal of Solids and Structures.* 1999;36(24): 3677–3708.
27. Teichmann FK, Wang C-T, Gerard G. Buckling of Sandwich Cylinders Under Axial Compression. *Journal of the Aeronautical Sciences.* 1951;18(6): 398–406.
28. Baker EH. Experimental investigation of sandwich cylinders and cones subjected to axial compression. *AIAA Journal.* 1968;6(9): 1769–1770.
29. Reese CD, Bert CW. Simplified design equations for buckling of axially compressed sandwich cylinders with orthotropic facings and core. *Journal of Aircraft.* 1969;6(6): 515–519.
30. Reese CD, Bert CW. Buckling of Orthotropic Sandwich Cylinders Under Axial Compression and Bending. *Journal of Aircraft.* 1974;11(4): 207–212.
31. Tennyson RC, Chan KC. Buckling of imperfect sandwich cylinders under axial compression. *International Journal of Solids and Structures.* 1990;26(9–10): 1017–1036.
32. Wicks N, Hutchinson JW. Optimal truss plates. *International Journal of Solids and Structures.* 2001;38(30–31): 5165–5183.
33. Valdevit L, Hutchinson JW, Evans AG. Structurally optimized sandwich panels with prismatic cores. *International Journal of Solids and Structures.* 2004;41(18-19): 5105–5124.
34. Liu T, Deng ZC, Lu TJ. Design optimization of truss-cored sandwiches with homogenization. *International Journal of Solids and Structures.* 2006;43(25-26): 7891–7918.
35. Liu T, Deng ZC, Lu TJ. Bi-functional optimization of actively cooled, pressurized hollow sandwich cylinders with prismatic cores. *Journal of the Mechanics and Physics of Solids.* 2007;55(12): 2565–2602.
36. Ghahfarokhi DS, Rahimi G. An analytical approach for global buckling of composite sandwich cylindrical shells with lattice cores. *International Journal of Solids and Structures.* 2018;146: 69–79.
37. Chen L, Zhang J, Du B, Zhou H, Liu H, Guo Y, Li W, Fang D. Dynamic crushing behavior and energy absorption of graded lattice cylindrical structure under axial impact load. *Thin-Walled Structures.* 2018;127: 333–343.
38. Jiang S, Sun F, Fan H. Multi-failure theory of composite orthogrid sandwich cylinder. *Aerospace Science and Technology.* 2017;70: 520–525.
39. Han Y, Wang P, Fan H, Sun F, Chen L, Fang D. Free vibration of CFRC lattice-core sandwich cylinder with attached mass. *Composites Science and Technology.* 2015;118: 226–235.

40. Zhang H, Sun F, Fan H, Chen H, Chen L, Fang D. Free vibration behaviors of carbon fiber reinforced lattice-core sandwich cylinder. *Composites Science and Technology.* 2014;100: 26–33.
41. Li W, Sun F, Wang P, Fan H, Fang D. A novel carbon fiber reinforced lattice truss sandwich cylinder: Fabrication and experiments. *Composites Part A: Applied Science and Manufacturing.* 2016;81: 313–322.
42. Zhang Z, Liu S, Tang Z. Crashworthiness investigation of kagome honeycomb sandwich cylindrical column under axial crushing loads. *Thin-Walled Structures.* 2010;48(1): 9–18.
43. Zhang Z, Liu S, Tang Z. Comparisons of honeycomb sandwich and foam-filled cylindrical columns under axial crushing loads. *Thin-Walled Structures.* 2011;49(9): 1071–1079.
44. Liu W, Lin Z, Wang N, Deng X. Dynamic performances of thin-walled tubes with star-shaped cross section under axial impact. *Thin-Walled Structures.* 2016;100: 25–37.
45. Su PB, Han B, Yang M, Wei XH, Zhao ZY, Zhang QC, Zhang Q, Qin KK, Lu TJ. Axial compressive collapse of ultralight corrugated sandwich cylindrical shells. *Materials & Design.* 2018;160: 325–337.
46. Wang E, Yao R, Li Q, Hu X, Sun G. Lightweight metallic cellular materials: a systematic review on mechanical characteristics and engineering applications. *International Journal of Mechanical Sciences.* 2024;270: 108795.
47. Santosa SP, Wierzbicki T, Hanssen AG, Langseth M. Experimental and numerical studies of foam-filled sections. *International Journal of Impact Engineering.* 2000;24(5): 509–534.